October 11, 2010

ERL option for LHeC

Y. Hao, D. Kayran, V.N. Litvinenko, V.Ptitsyn, D. Trbojevic, N. Tsoupas

C-AD, Brookhaven National Laboratory, Upton, NY 11973, USA

Introduction

In this document we summarize a set of self-consistent system for a 3-pass 60 GeV energy recovery linac. We use racetrack configuration for the system with the beam parameters specified in IPAC'10 paper: *Designs for a Linac-Ring LHeC, F. Zimmermann et al., Proceedings of First International Particle Accelerator Conference, IPAC'10, Kyoto, Japan from Sunday to Friday, May 23-28, 2010, pp. 1611-1613,* *http://accelconf.web.cern.ch/AccelConf/IPAC10/papers/tupeb039.pdf*

Table 1. Lepton Beam Parameters and Luminosity

e− energy at IP [GeV]	60
Luminosity [10^{32} $cm^{-2}s^{-1}$]	10.1
Polarization (%)	90
Bunch population [10^9]	2.0
e− bunch length [μm]	300
Bunch interval [ns]	50
Transv. emit. $\gamma\varepsilon_{x,y}$ [μm]	50
Rms IP beam size [μm]	7
Hourglass reduction H_{hg}	0.91
Crossing angle θc	0
Repetition rate [Hz]	CW
Average current [mA]	6.6
ER efficiency η	94
Total wall plug power [MW]	100

In addition, we used average arc radius of 1 km and injection energy of 0.3 GeV. The 0^{th} order acceleration/deceleration scenario then looks as following:

Table 2. Acceleration/deceleration scenario: Injection energy is 0.3 GeV with an energy gain per linac 9.95 GeV.

Pass	Arc 1	Arc 2
1	10.25	20.20
2	30.15	40.10
3	50.05	**60.00**
4	50.05	40.10
5	30.15	20.20
6	10.25	0.30

Synchrotron radiation is significant factor and has to be taken into the account.

We suggest using eRHIC-type cryo-module with six 703 MHz SRF 5-cell cavities as a main linac's unit for such ERL.

We present here the lattice of arcs, mergers/combiners and linac, the evolution of the beam parameters under synchrotron radiation, two options for compensating the synchrotron radiation losses; and an estimation of CSR and resistive wall losses/energy spread growth.

We are presently working on a TBBU simulations for such system.

1. Arc's lattice

Arc lattice is the starting point for the layout design of the ERL because it determines the radius of the curvature in the dipole magnets and the all-important losses on synchrotron radiation, which have to be compensated.

Similar to eRHIC design, we suggest using economic option of small gap magnets (with gap as small as 0.5 cm). It provides for low cost, low power consumption, high gradients in normal-conducting quadrupoles, and for very compact arcs.

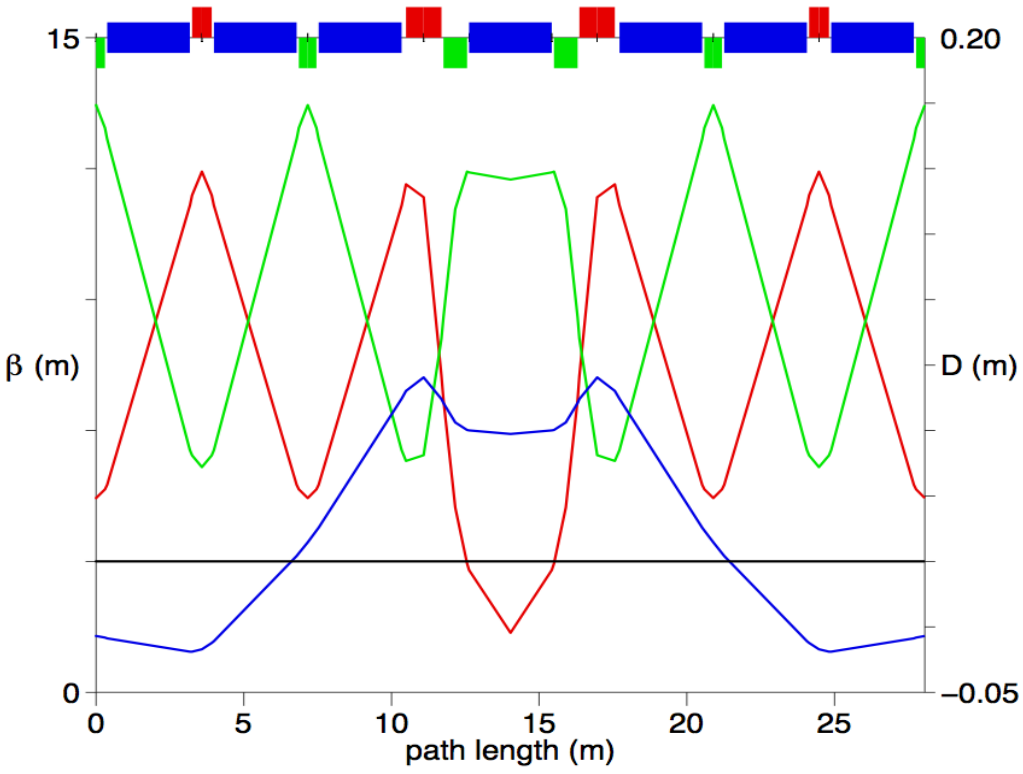

Fig. 1.1 Regular isochronous lattice of ERL's arcs. Length of cell is 27.8017 m. Red line – horizontal β-function, green - vertical β-function, blue – dispersion.

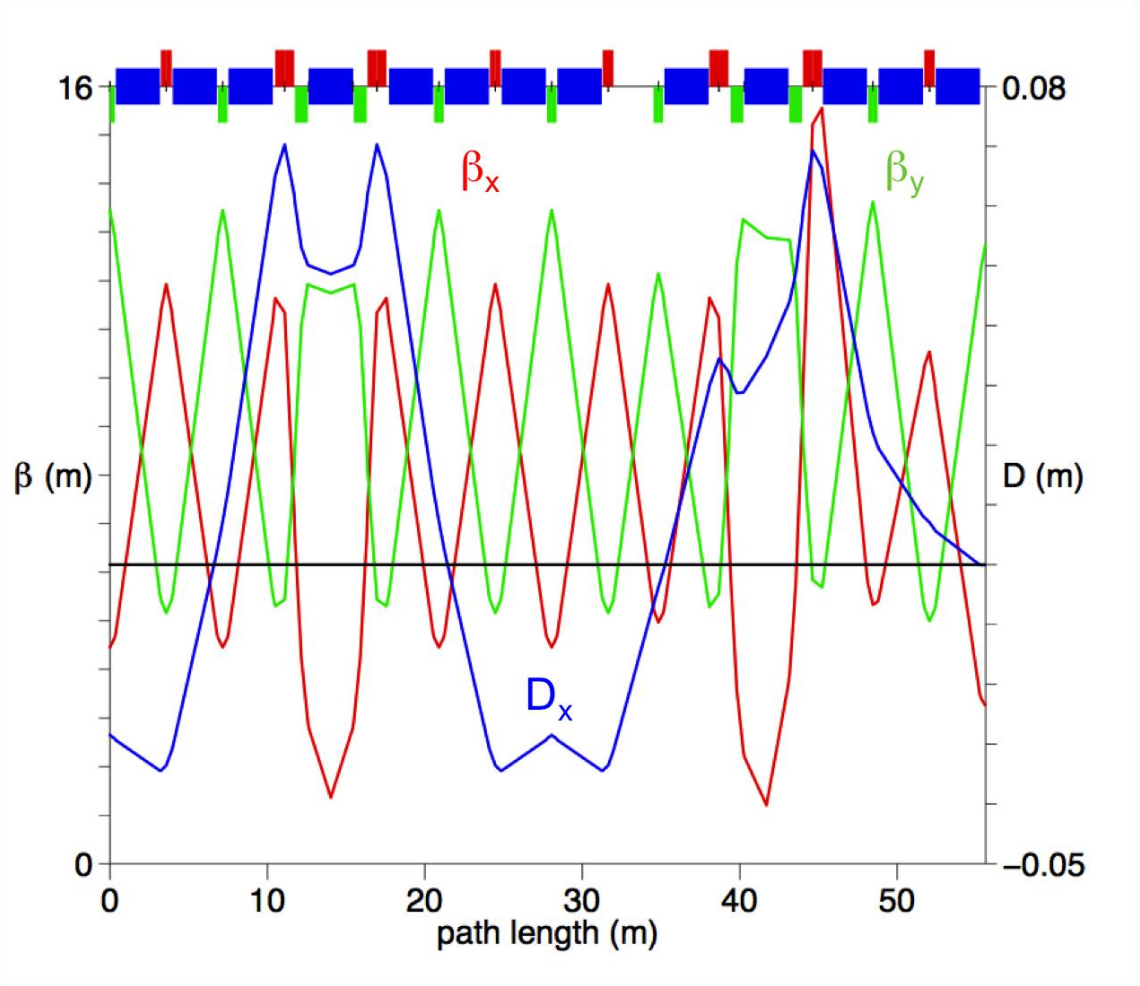

Fig. 1.2. The regular and the end of the arc cell lattice.

This lattice has a number of advantages. It has small β-functions (maxima are 13.1 m horizontally and 12.7 m vertically) and the dispersion-function (D_{max}= 0.063 m, D_{min}= -0.031 m), which ultimately provide for a very small beam size in the arcs: the horizontal RMS size measures 94 microns at the top energy and 313 microns in the 10 GeV arc during the recovery cycle. Similarly, the vertical RMS size measures 74 micron in 60 GeV arc and 178 micron in the 10 GeV arc. Hence, the aperture of the arc's vacuum chambers and the arc's magnets can be only few millimeters.

A 180-degree arc (with average radius of 1000 m) consists of 113 asynchronous arc cells with length of 27.8017 m[1]. As shown below, this lattice provides sufficiently low emittance growth. We consider that control of R_{56} in such ERL is of critical importance and using an asynchronous arc lattice with R_{56} controllable around near-zero value is important for keeping the energy spread, the recirculation/recovery and the energy spread under control. This consideration came as a result of detailed studies for eRHIC ERL. One of the most important features of this lattice is that it has excellent filling factor, while R_{56} can be made either zero, slightly positive or slightly negative. The arc can be turned into achromatic by the use of slightly modified end cells as shown in Fig. 1.2 .

[1] A similar lattice with a half-length was developed to reduce the emittance growth by an order of magnitude. It could be used if emittance reduction is needed.

Here and further on we are giving parameters of magnetic elements for 60 GeV arc, where their strength are maximal. The other arcs have identical lattice, but the strength of the elements is reduced proportionally with the Bro of the beam.

Each arc comprised of seven dipole magnets, four focusing and five defocusing quadrupoles. One of the later is shared between two neighboring cells. No sextupoles are used in this ERL. All dipoles are identical and have length of 2.8 m. The filling factor in this lattice is 69.7%, the bending radius is 697 m and the maximum bending field is 0.287 T in the 60 GeV arc.

The quadrupoles in the regular arc cell have the following parameters:

Table 3. Quadrupoles parameters:

Name	Length (m)	Gradient (T/m)
QF0	0.665	84.975
QD0	0.600	-88.970
QF3	1.200	107.75
QD3	0.800	-103/89
QF3S	1.200	107.220
QD3S	0.800	-101.095

In the matching cell to the arc, in addition to the regular quadrupoles QF0 and QD0 two "doublet" quads are QF3S and QD3S, as shown in the Table 3. Other details of the lattice are in the Table 4.

Hence, A 180-degree arc contains 782 dipoles and 1017 quadrupoles. Four quadrupole families are fed in series.

The integral for the 360-degrees are as follows: I1 = 0.19008E-01, I2 = 0.89124E-02, I3 = 0.12642E-04, I4 = 0.38244E-07, I5X = 0.10262E-07.

Using formulae for the growth of the normalized emittance and the energy spread

$$\varepsilon_n = \varepsilon_{no} + \frac{55}{24\sqrt{3}}\Lambda_c r_e \int \frac{\gamma^6(s)}{\rho^3(s)} H(s)ds; \quad H(s) = \frac{D^2 + (D'\beta + \alpha D)^2}{\beta}, \qquad (1)$$

and

$$\left\langle \delta\gamma^2 \right\rangle = \left\langle \delta\gamma^2 \right\rangle + \frac{55}{24\sqrt{3}}\Lambda_c r_e \int \frac{\gamma^7(s)}{\rho^3(s)} ds; \quad \frac{55}{24\sqrt{3}}\Lambda_c r_e = 1.439754 \cdot 10^{-27} m^2 \qquad (2)$$

we get that during the acceleration of the beam to 60 GeV (i.e. before it collides) the horizontal normalized emittance grows by 8.59 mm mrad and its RMS energy spread adds 15.98 MeV. The total normalized emittance growth from the moment of injection to its ejection measures 36.53 mm mrad. The RMS energy spread adds to 35.24 MeV, i.e.

the beam is ejected with 11.7% energy spread. Further details of the emittance and energy spread evolution are given in Table 5.

Table 4. Detailed list of the lattice parameters: The table extends to the point of bilateral symmetry in the center of the cell.

L,m	Element	s(m)	βx(m)	βy(m)	D(m)	αx	αy	D'	NUX	NUY
0	0	0	12.68	-0.03	0	0	0	0	0	5.27068
0.3	QD2	0.3	5.50	12.19	-0.02652	-0.77102	1.60348	-0.00345	0.00893	0.00381
0.075	O	0.375	5.62	11.95	-0.02677	-0.79277	1.58151	-0.00345	0.01108	0.0048
2.8	B2	3.175	12.33	5.39	-0.03086	-1.60459	0.76149	0.00052	0.0657	0.06149
0.075	O	3.25	12.57	5.28	-0.03083	-1.62633	0.73953	0.00052	0.06666	0.06372
0.3325	QF2	3.5825	13.12	5.04	-0.02999	0	0	0.00448	0.07075	0.07406
0.3325	QF2	3.915	12.57	5.28	-0.02787	1.62633	-0.73953	0.00824	0.07484	0.0844
0.075	O	3.99	12.33	5.39	-0.02725	1.60459	-0.76149	0.00824	0.0758	0.08663
2.8	B2	6.79	5.62	11.95	0.00138	0.79277	-1.58151	0.01221	0.13042	0.14332
0.075	O	6.865	5.50	12.19	0.00229	0.77102	-1.60348	0.01221	0.13257	0.14431
0.3	QD2	7.165	5.27	12.68	0.00602	0	0	0.01276	0.1415	0.14812
0.3	QD2	7.465	5.50	12.19	0.01	-0.77102	1.60348	0.01381	0.15043	0.15193
0.075	O	7.54	5.62	11.95	0.01103	-0.79277	1.58151	0.01381	0.15258	0.15292
2.8	B2	10.34	12.33	5.39	0.05525	-1.60459	0.76149	0.01778	0.2072	0.20961
0.1928	OFW	10.5328	12.96	5.11	0.05868	-1.66049	0.70503	0.01778	0.20963	0.21545
0.54	QF3	11.0728	12.38	5.34	0.06267	2.67097	-1.16173	-0.00323	0.21621	0.23243
0.54	QF3	11.6128	7.87	7.94	0.0553	5.15354	-3.93768	-0.02365	0.22466	0.24605
0.0879	O1F	11.7007	6.99	8.65	0.05322	4.84558	-4.12051	-0.02365	0.22654	0.24774
0.32	QD3	12.0207	4.62	10.76	0.04749	2.7339	-2.31721	-0.01237	0.23561	0.25296
0.32	QD3	12.3407	3.32	11.47	0.04521	1.42995	0.13857	-0.00199	0.24878	0.25749
0.1602	O2F	12.5009	2.89	11.43	0.04489	1.2832	0.12435	-0.00199	0.25701	0.25971
1.4	B2SH	13.9009	1.09	11.26	0.0435	0	0	0	0.40165	0.2794

During their trip from the injection to ejection the electrons lose 2.05 GeV of their energy to the synchrotron radiation (0.813 GeV of which occurs in 180-degree of the 60 GeV arc). For 6.6 mA electron beam, the 13.54 MW of the lost power should be compensated (see later section).

Overall, the arc lattice provides the necessary beam parameters for the LHeC.

Table 5. Emittance and energy spread growth in the ERL's arcs caused by quantum fluctuations of synchrotron radiation

Arc	**E, GeV**	**γ**	**δE, SR, GeV**	**δεn, m rad**	**$\delta\gamma^2$**	***total***	***σγ/γ***
1	10.25	2.01E+04	6.93E-04	4.81E-10	1.19E-02	1.19E-02	5.44E-06
2	20.2	3.95E+04	1.04E-02	2.82E-08	1.37E+00	1.38E+00	2.98E-05
3	30.15	5.90E+04	5.18E-02	3.12E-07	2.27E+01	2.40E+01	8.31E-05
4	40.1	7.85E+04	1.62E-01	1.73E-06	1.67E+02	1.91E+02	1.76E-04
5	50.05	9.79E+04	3.94E-01	6.52E-06	7.87E+02	9.78E+02	3.19E-04
6	60	1.17E+05	8.13E-01	1.94E-05	2.80E+03	3.78E+03	5.23E-04
5	50.05	9.79E+04	3.94E-01	6.52E-06	7.87E+02	4.56E+03	6.90E-04
4	40.1	7.85E+04	1.62E-01	1.73E-06	1.67E+02	4.73E+03	8.77E-04
3	30.15	5.90E+04	5.18E-02	3.12E-07	2.27E+01	4.75E+03	1.17E-03
2	20.2	3.95E+04	1.04E-02	2.82E-08	1.37E+00	4.76E+03	1.74E-03
1	10.25	2.01E+04	6.93E-04	4.81E-10	1.19E-02	4.76E+03	3.44E-03
Total			**2.05E+00**	**3.65E-05**	**4.76E+03**		

2. Linac lattice

The linac lattice is defined to a large degree by its SRF cavities. As we mentioned above, we assume that the injection energy is 0.3GeV and the energy gain per linac is 9.95GeV and the top energy in the collision point is 60 GeV. After the collision the beam is decelerated in the same linacs towards the injection energy.

We suggest using eRHIC type 9.6 m long cryo-modules with length of 9.6 m (as shown in Fig. 2.1). The module is comprised of six SRF 703 MHz 5-cell cavities. The 9.95 GeV linac will requires 80 modules with a total length of 800 m. The energy gain per 5-cell cavity will be 20.73 MeV.

Our detailed studies showed that with the very large ratio between the injection energy (0.3 GeV) and the linac energy gain (~ 10 GeV) the use of quadrupoles in the linacs do not provide additional (any significant) benefit. In other terms, the average β-functions in the linacs not reduce significantly compared with the straight linac without quadrupole focusing. Furthermore, necessity of elongating linac to provide space for quadrupoles seems to be contra-productive.

Hence, unless linacs are split into *n* smaller sections (this requires use of additional splitters and combiners with multiple 3*n* beam-lines), there is no significant gain by using quadrupoles. The splitting linacs would provide proportional reduction of the maximum of the beta-functions. But, it would become a significant complication of the system (with *3n* additional focusing channels) and may cause significant cost increase.

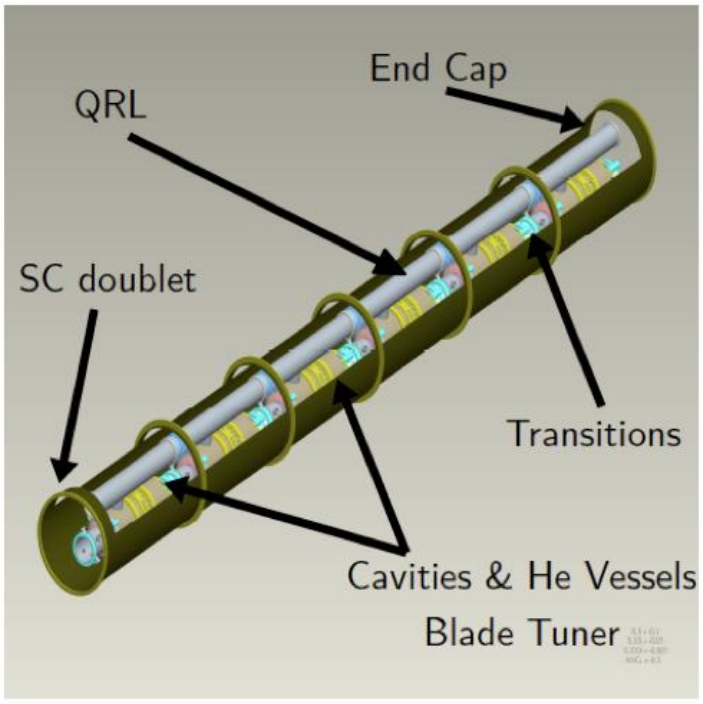

Fig.2.1. The eRHIC-type cryo-module containing six 5-cell SRF 703 MHz cavities.

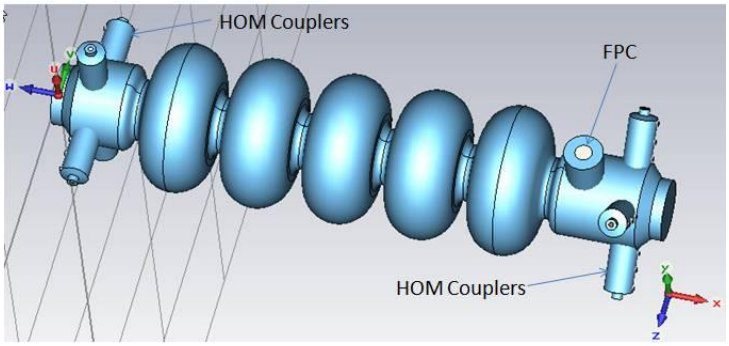

Fig.2.2. Model of a new 5-cell HOM-damped SRF 703 MHz cavity.

While designing the linac lattice we took into account focusing provided by the RF system. As shown in Fig. 2.3, the field profile in BNL's 5-cell cavity is very close to the standing wave:

$$E_o(z,t) \cong E_o \sin k_{rf} x \cdot \sin \omega_{rf} t; \quad \omega_{rf} = c k_{rf} \tag{3}$$

which provides alternating gradient focusing as

$$\begin{aligned} \frac{dx}{dt} &= \approx \frac{p_x}{mc\left(\gamma_o + \gamma' z\right)}, \\ \frac{1}{mc}\frac{dp_x}{dz} &= -2k_{rf}\gamma' \frac{\sin\left(2k_{rf} z + \varphi_0\right)}{\cos\varphi_0} \cdot x \end{aligned} \tag{4}$$

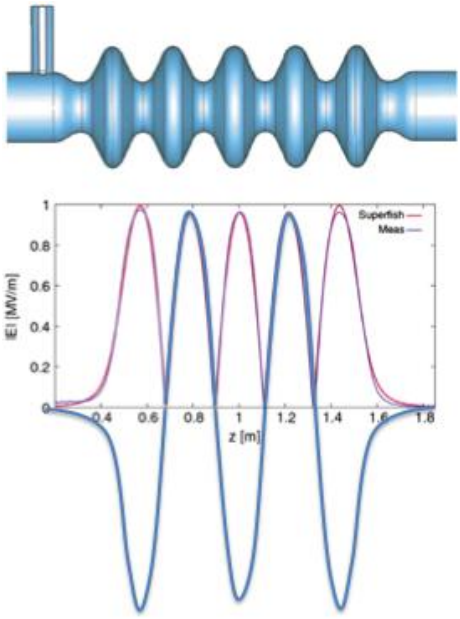

Fig.2.3. Field profile in BNL's 5-cell cavity: the cyan curve shows the absolute value of the peak electric field along axis; the light blue curve shows the electric filed on the axis at t=0 (zero phase).

Two thin lenses per cell approximation by the RF focusing could be shown as:

$$\frac{1}{mc}\Delta p_x = -x(z)\cdot\frac{(-1)^n}{\cos\varphi_0}\gamma'\int_0^{\pi}\sin(\theta+\varphi_0)d\theta = -2\cdot(-1)^n x(z)\cdot\gamma' \qquad (5)$$

The optimized β-functions for the entire ERL are shown in Fig.2.4 – here we show only linacs. The sets of "splitter-arc-combiner" connect the linacs and provide the matching of β-functions and α-functions between linacs. The corresponding β-functions and α-functions at the ends of the linacs are listed in the following table:

Table 6. The β and α-functions at the ends of the linacs.

# of pass in linac	β (entr.)	α (entr.)	β (exit)	α (exit)
1	294.6	-1.14	769.3	-1.18
2	898.1	1.89	905.3	-1.53
3	915.4	1.84	916.7	-1.61
4	919.7	1.81	920.0	-1.65
5	921.4	1.79	921.6	-1.67
6	922.3	1.78	922.2	-1.68

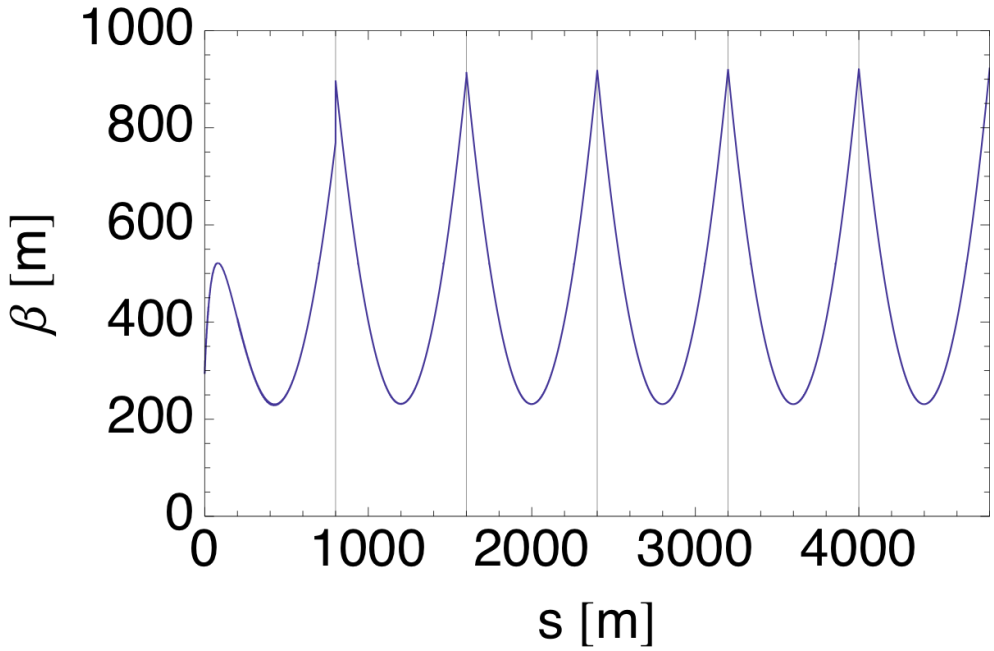

Fig.2.4. The β-functions of the ERL linacs during acceleration from 0.3 GeV to 60 GeV. The figure is a simple mirror image during the deceleration cycle. The splitters, the ARCS and the combiners, which connect the two linacs have been omitted from the plot of the beta functions. They are located at the vertical lines of the plot.

3. Lattice of splitters and combiners.

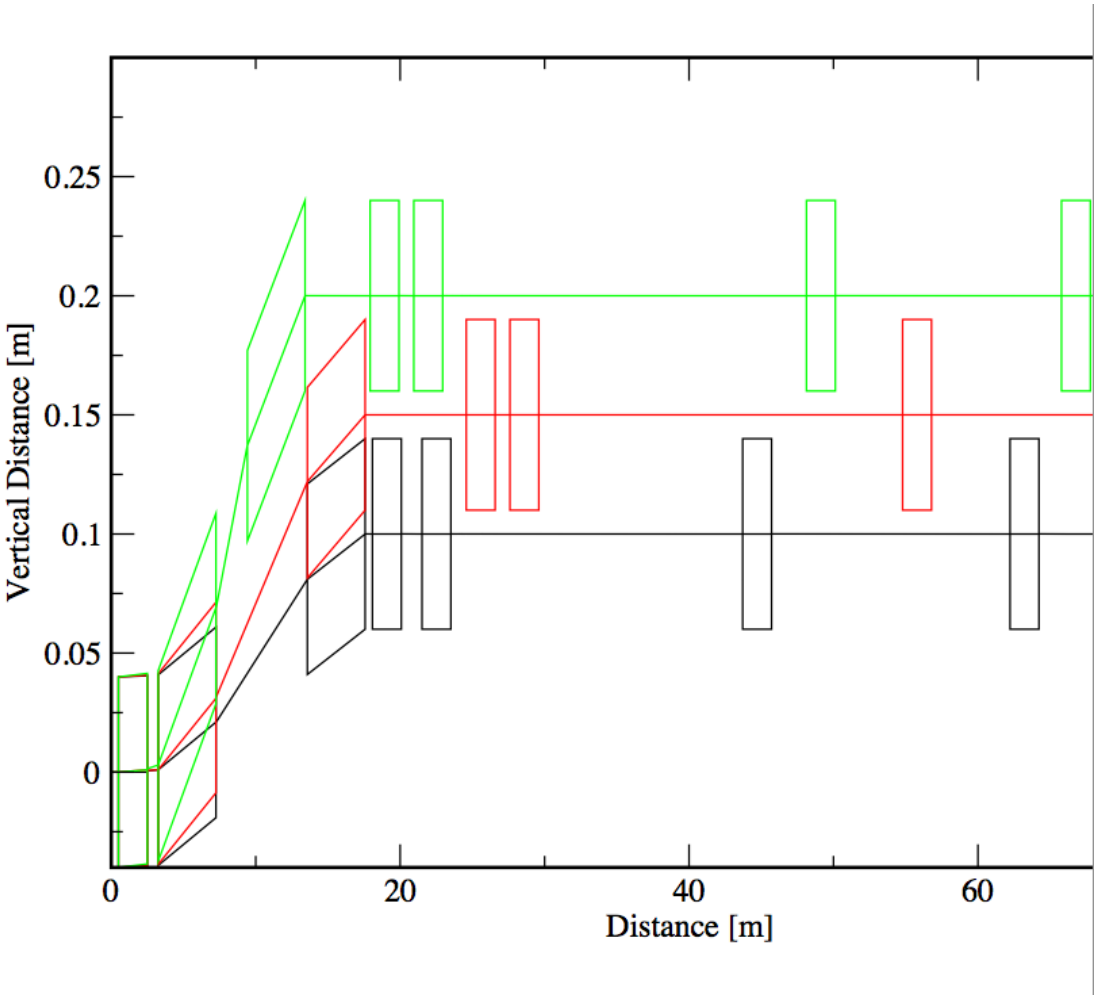

Fig. 3.1. The vertical splitter after first linac. The combiner looks as a mirror image of the splitter. The first green rectangle in the figure serves as a low field dipole for the beam injection of the 0.3 GeV beam into the first linac. It does not affect significantly the much higher circulating beams in the racetrack ERL's linacs

The splitters and combiners play a dual role in the lattice. First, they either separate or combine three (or four) beams with different energies. Second, they match the lattice of linac with that of the arcs.

We suggest separating the arcs vertically by 5 cm as shown in Fig. 3.1. Small separation is important because it can be provided at a modest distance by 10 mrad magnets. Fig. 3.2 shows the matching of the linac optics into that of the arc.

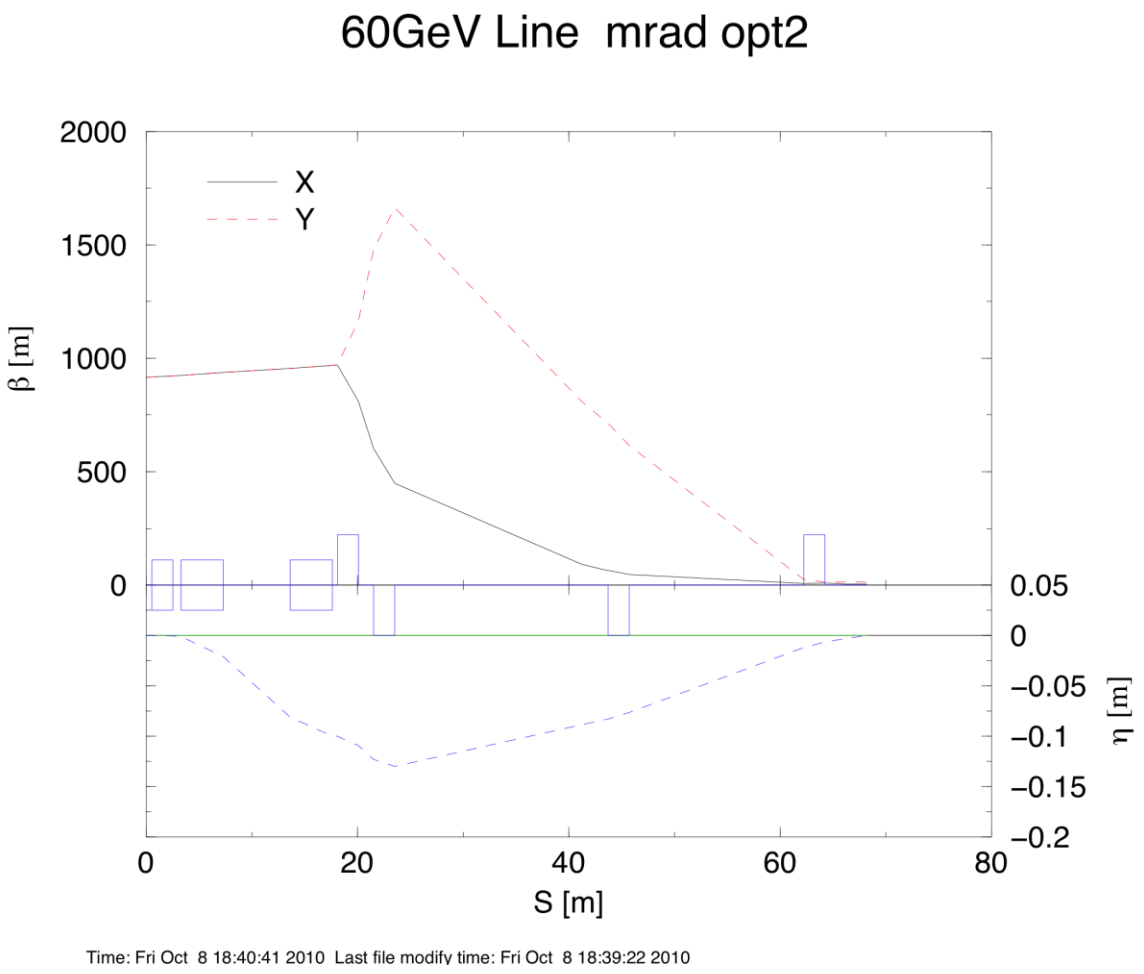

Fig. 3.2. Optics functions of splitter for 20, 40 and 60 GeV beams and matching with the arc.

Overall, the 70-m long splitters and combiners provide both geometrical and optics matching of the arcs and the linacs.

4. IR lattice.

The IR lattice is developed by CERN team and it should be matched with the neighboring sections of the lattice.

5. Layout and compensation of synchrotron radiation losses

For 6.6 mA electron beam, the 13.54 MW of the lost power should be compensated. We discuss here two possible schemes

5.1. Using second harmonic RF

A simple-minded layout of the ERL-based LHeC is shown in Fig. 5.1.

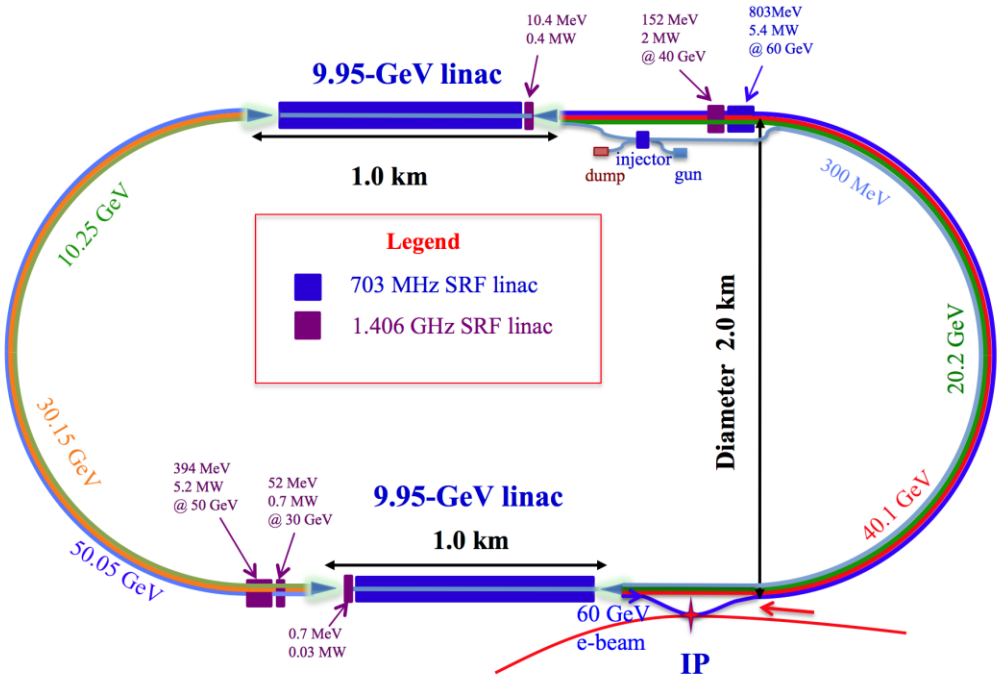

Fig. 5.1. Layout of racetrack 60 GeV ERL.

The footprint of the accelerator is 2 km x 3.5 km. It can be a bit longer, depending on IR straight length. Legend: blue rectangles – SRF linacs at 703 MHz, magenta rectangles – second harmonic 1.406 GHz SRF cavities.

Polarized electrons from the electron gun are accelerated to 300 MeV in the injector linacs and are injected into the racetrack ERL with two 9.95 GeV linacs. Electrons are accelerated to 60 GeV in 3 passes and then decelerated back to 300 MeV before being ejected into the injector. They are further decelerated in the injector could can have similar design as the eRHIC's pre-injector.

In this scheme, two main 9.95 GeV linacs work in the complete energy recovery mode and all bunches are accelerated and decelerated on-crest. Energy loss due to the synchrotron radiation is compensated by six additional linacs. A 703 MHz 803 MeV linac compensates for majority of the losses in the 60-GeV arc. The remaining energy loss of 10.4 MeV is taken care of by a common second harmonic cavity in the first linac 1 (on the top of the figure 5.1). The second harmonic cavities with energy gains of 394 MeV, 152 MeV and 53 MeV are used in for the 30 GeV, 40 GeV and 50 GeV arcs, correspondingly. Two second order harmonic cavities with energy gains of 0.7 MeV and 10.4 MeV are installed together with the main linacs and are passed through by all beams.

The second harmonic RF gives equal (positive) energy boosts for both the accelerating and the decelerating beams passing through the five arcs. The 60 GeV arc is the only arc

where the beam passes only once – hence, we can use fundamental RF for compensating the energy loss.

Additional losses coming from HOM, restive wall and CSR depend on the choice of the linac, the peak current and the design and material of the vacuum chamber. They will modify energy losses, which can be accommodated within the framework of this scheme by changing voltages of the loss-compensating RF systems.

Although this scheme is straightforward, it requires six additional SRF linacs. Beside the need of both fundamental and second harmonic SRF linacs, these linacs have different loads and therefore require three different couplers.

More importantly, four of these cavities are installed at individual arcs. Hence, the beams passing through the other arcs should be diverted around these linacs. These bypasses are an additional complication of this scheme.

The bottom line – in this scheme one needs to install additional 1.412 GeV of SRF linacs for compensating the SR losses.

5.2. Compensating for SR by the main linacs

A new approach using the main linacs for compensating the energy losses in the arcs was recently developed. This scheme provides identical energies of the accelerating and the decelerating bunches propagating in the same arc. The mathematics is shown in Appendix 1 – a paper on this subject will be sent for publication soon. The Mathematica is used to solve the chain of equations.

Using the same RF linacs for ERL and the energy loss compensation has a number of advantages. First, each of 1,000 RF transmitters driving individual 5-cell cavity have power ~ 5-10 kW to compensate for micro-phonics noise. Adding 12 to 15 kW load per unit will not only compensate for the losses, but would also provide natural reduction of Q_{ext}. Furthermore, there will be only one type of a cavity with one type of a coupler. Finally, as we show below it will require only 0.45 GeV of additional linac.

The only potential drawback is that the beams are passing the cavities off-crest. At the same time, this is a typical mode of SRF cavities operation in the high-energy electron storage rings.

Here we present one of reasonably good solutions, with the layout shown in Fig. 5.2.

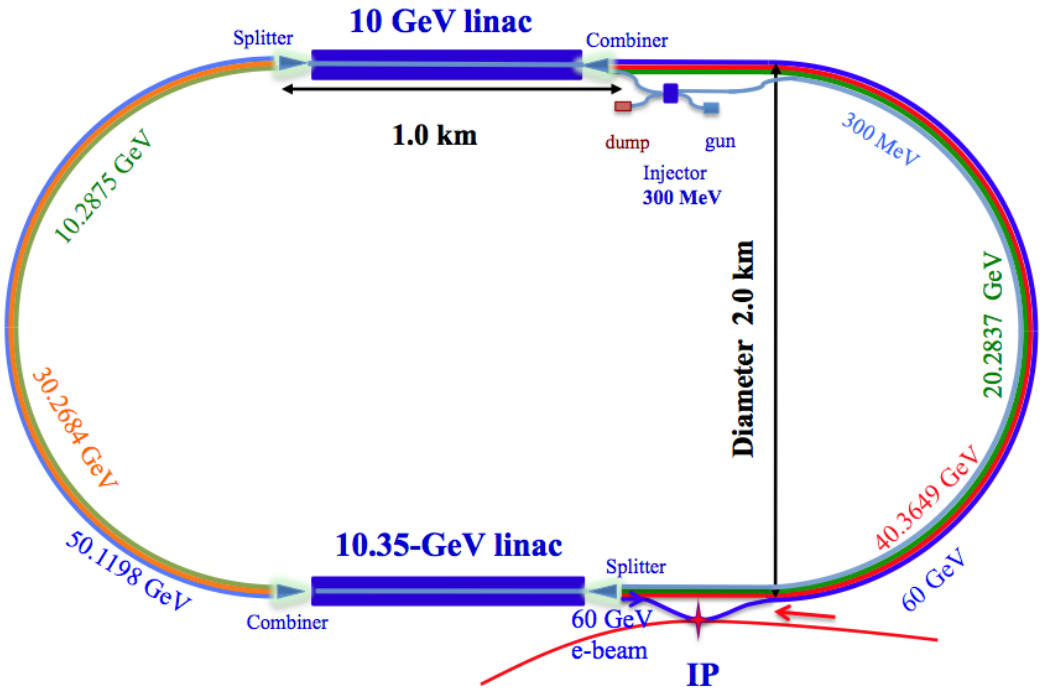

Fig. 5.2 Layout of LHeC's 60 GeV with SR losses compensation in main linacs.

In this scheme the arc's lengths (pass time) differ slightly from the integer number of the RF wavelength (RF periods). The Table 7 shows the initial phase, the phase advances (modular 2π) in the individual arcs. As we mentioned above, in each arc the energy of the beam is the same on the way up and on the ways down. It is also true about the phase advances. Finally, the beam is ejected at energy of 300 MeV to be decelerated further in the injector linac to 5-10 MeV and to be dumped.

Table 7. The initial phase and phase advance in the individual arcs

	Phase, radians	Comment
Injection phase	-0.05	$\varphi 1$, injection phase
10.2875 GeV arc	-0.211966	$\Delta\varphi 1$, phase advance
20.2837 GeV arc	0.231414	$\Delta\varphi 2$, phase advance
30.2687 GeV arc	-0.166757	$\Delta\varphi 3$, phase advance
40.3649 GeV arc	0.322776	$\Delta\varphi 4$, phase advance
50.3649 GeV arc	-0.00580018	$\Delta\varphi 5$, phase advance
60 GeV arc	2.586565	$\Delta\varphi 6$, phase advance

The electron bunch passes through the main linacs twelve times in the following sequence of phases: -0.05, -0.261966, -0.0305519, -0.197309, 0.125467, 0.119667, 3.08786, 2.85644, 3.0232, 2.70042, 2.70622, 2.87589. Finally, linac 1 will compensate

for 0.922 GeV of the energy loss, while the linac 2 will compensate for the remaining 1.144 GeV.

Table 8 details the results of direct tracking of the e-beam in such system. It shows phases, energy gains and losses when beam traverses the ERL from the injection to ejection. It is a specific practical prove that such system can be

Table. 8. Phase and energy of a beam in 60 GeV ERL with SR losses compensation by its main linacs.

Process	Initial energy	Phase, rad	Acceleration deceleration	SR loss	Final energy
Linac 1	0.300	**-0.05**	9.987502604		**10.288**
Arc 1	10.288	**-0.211966**		0.000702628	10.287
Linac 2	10.287	-0.261966	9.996885846		**20.284**
Arc 2	20.284	**0.231414**		0.010618741	20.273
Linac 1	20.273	-0.030552	9.99533324		**30.268**
Arc 3	30.268	**-0.166757**		0.052655461	30.216
Linac 2	30.216	-0.197309	10.14918565		**40.365**
Arc 4	40.365	**0.322776**		0.166533796	40.198
Linac 1	40.198	0.125467	9.921393359		**50.120**
Arc 5	50.120	**-0.00580018**		0.395842588	49.724
Linac 2	49.724	0.11966682	10.27598163		**60.000**
Arc 6	60.000	**2.586495**		0.812996158	59.187
Linac 1	59.187	2.70616182	-9.066884004		**50.120**
Arc 5	50.120	**-0.00580018**		0.395850766	49.724
Linac 2	49.724	2.70036164	-9.35874573		**40.365**
Arc 4	40.365	**0.322776**		0.166542409	40.199
Linac 1	40.199	3.02313764	-9.929924046		**30.269**
Arc 3	30.269	**-0.166757**		0.052659537	30.216
Linac 2	30.216	2.85638064	-9.931880927		**20.284**
Arc 2	20.284	**0.231414**		0.010620332	20.274
Linac 1	20.274	3.08779464	-9.985532359		**10.288**
Arc 1	10.288	**-0.211966**		0.000702844	10.288
Linac 2	10.288	2.87582864	-9.986633411		0.301
Ejection	0.301			5.14637E-10	0.301

We have showed by tracking particles with initial RMS bunch length of 0.3 mm and the RMS energy spread of 50 keV through the ERL does not cause any significant energy spread (chirp) growth. The phase-correlated relative energy spread stays below 10^{-4} and is equal 3.8 10-5 in the collision point at 60 GeV. On the way down the spread does increase to 3.8 10-4 at 10 GeV energy. It is at 0.3% when ejected from the ERL into the injection linac.

In absolute value, at the ejection the correlated RMS energy spread is 820 KeV, while the uncorrelated energy spread induced by quantum fluctuation of synchrotron radiation is 35.3 MeV. Hence, the correlated energy spread from the off-crest crossing is significantly smaller than the uncorrelated energy spread induced by the SR. As we will see in the next chapter, it is also much smaller than the correlated spread induced by wake fields.

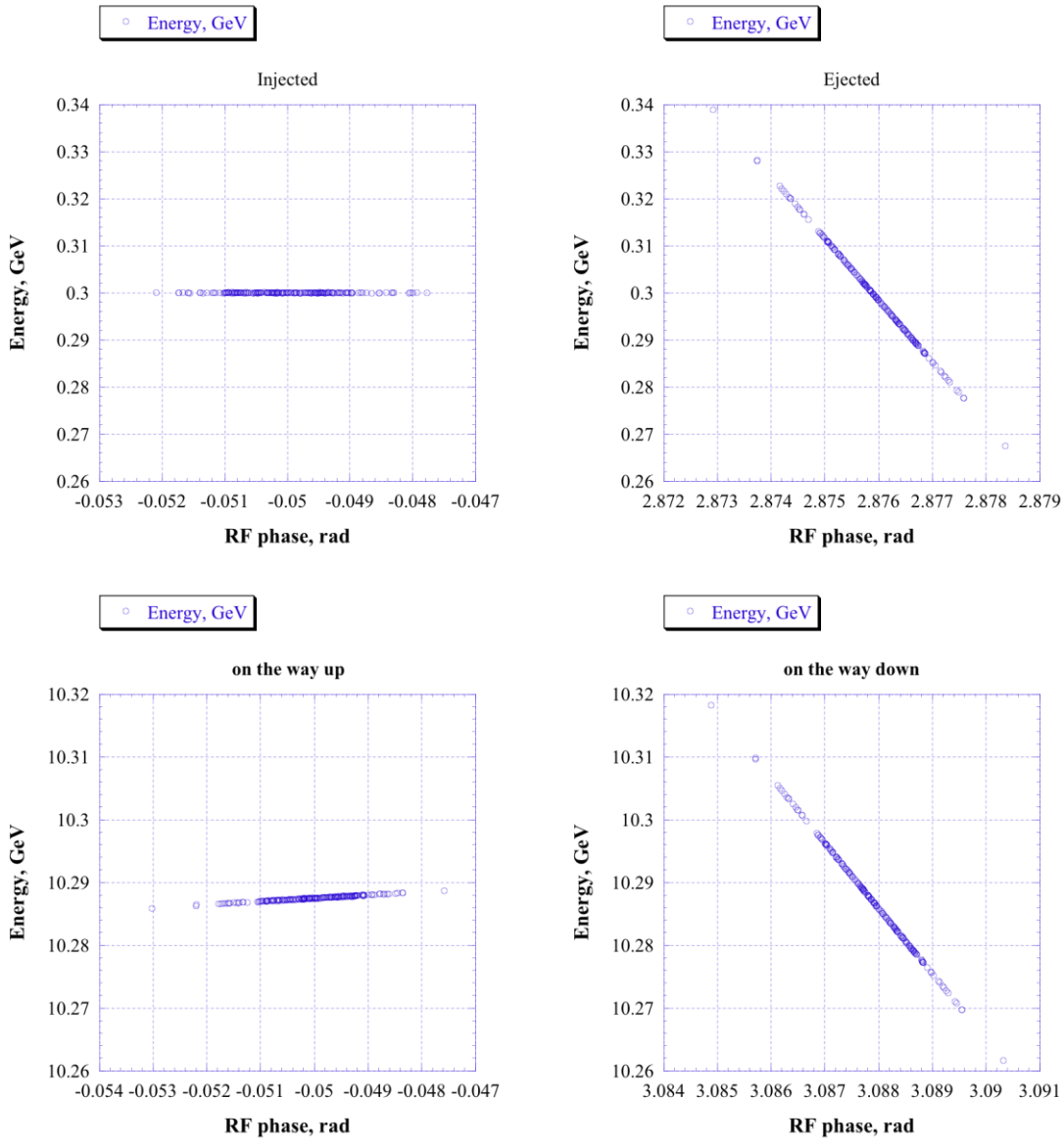

Fig. 5.3 Phase space at lowest energies

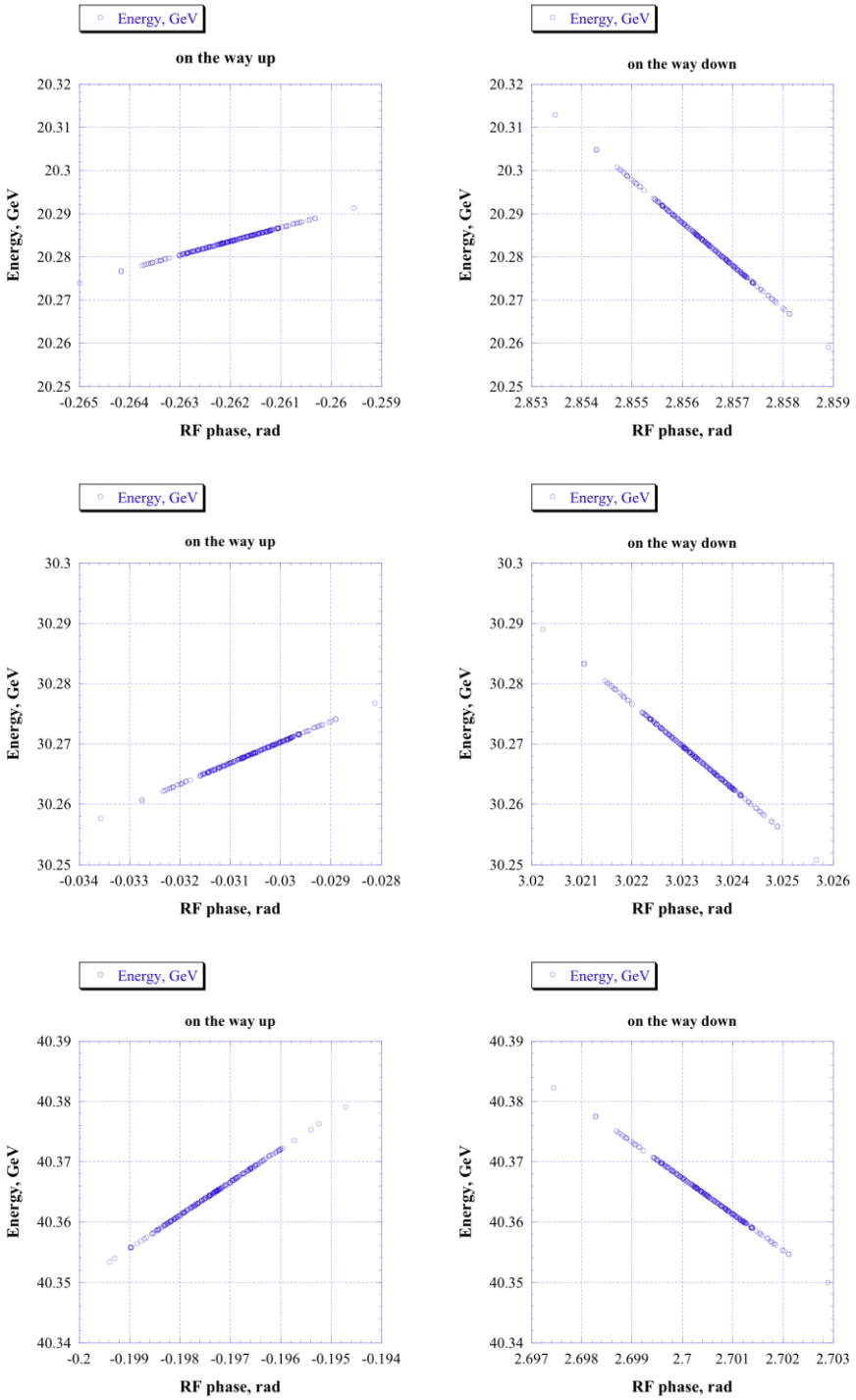

Fig. 5.4 Phase space at medium energies

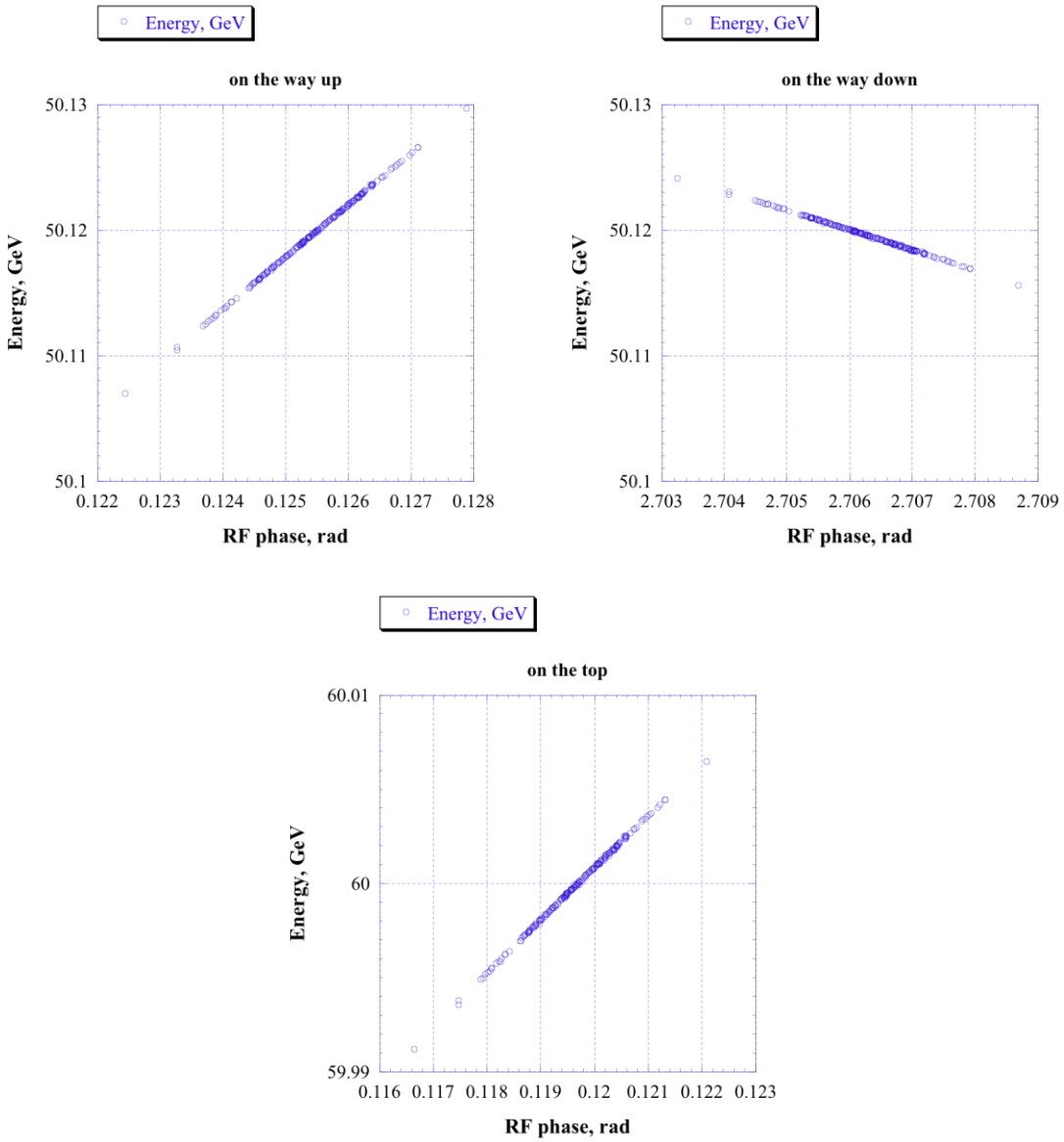

Fig. 5.5 Phase space at top energies

Both economically and conceptually, this can be a better choice for the ERL. In addition, full control of the value and the sign of R_{56} in each arc will allow us to manipulate the longitudinal phase space and to reduce the energy spread at the ejection.

6. Coherent energy losses

Two types of losses has been studied: a) resistive wall, b) coherent synchrotron radiation. Following parameters were used for the calculations:

Bunch length	0.3mm
Number of electrons per bunch	2 10^9
Average arc v	1000 m
Bending radius	697 m

The resistive wall losses per one 180-degree arc are shown in Fig. 6.1. We suggest using small gap extruded Al vacuum chambers with the full gap of 4 mm.

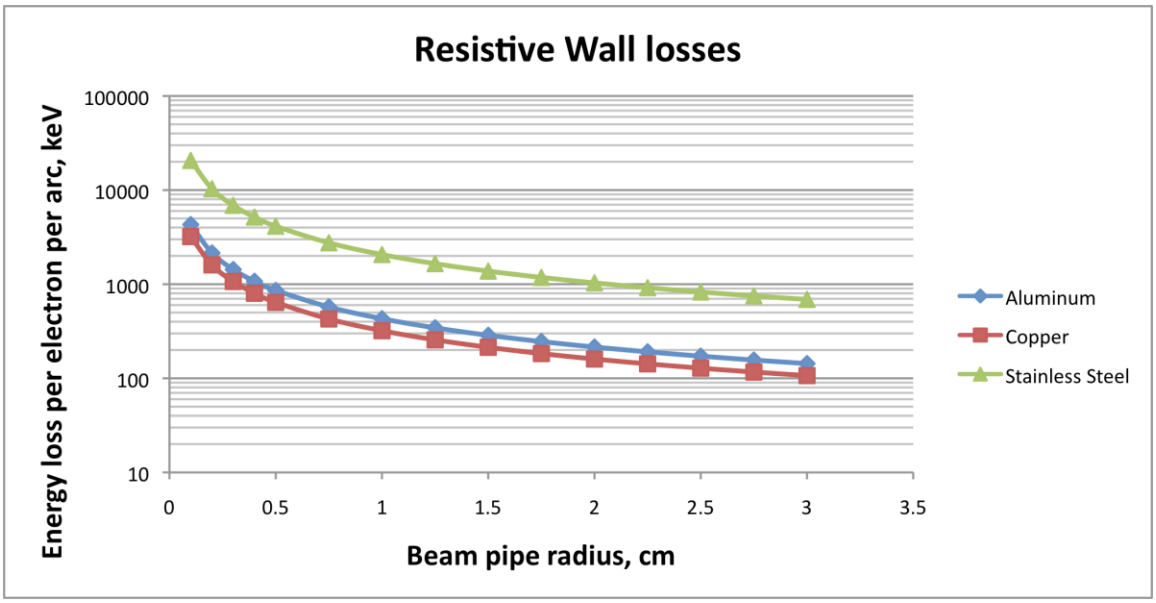

Fig. 6.1 Loss of the beam energy per 180-degree arc in LHeC ERL for three different

With the effective Al pipe radius ~ 2 mm there will be additional 24 MeV energy loss and similar level of the energy spread due to the resistive wall. While 24 MeV energy loss is very small compared with 2.05 GeV SR loss, the induced correlated energy spread is comparable with the 35 MeV RMS uncorrelated spread induced by SR.

Without shielding, the beam will loose 1.4 MeV per arc due to Coherent Synchrotron Radiation (CSR). Again, it is dwarfed by the incoherent SR losses. The total induced correlated energy spread will be about 12 MeV.

In any case, the CSR will be strongly suppressed by the walls of the vacuum chamber. Corresponding suppression factor is shown in Fig. 6.2

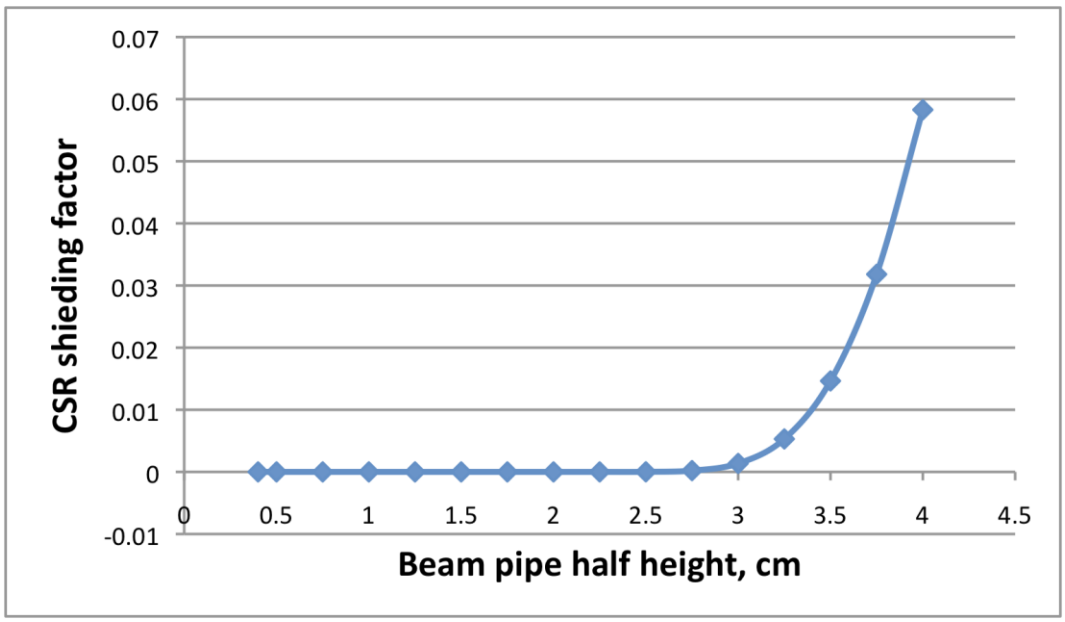

Fig. 6.2 CSR shielding factor by the beam pipe

7. TBBU estimations

For BBU simulation we use 70 dipole High Order Modes (HOMs) based on simulation and measurements of BNL 5cell cavity (see Fig. 7.1 and 10 the largest (R/Q)*Q are presented in table Table 8). Each HOM has either 0 or 90 degrees polarization.

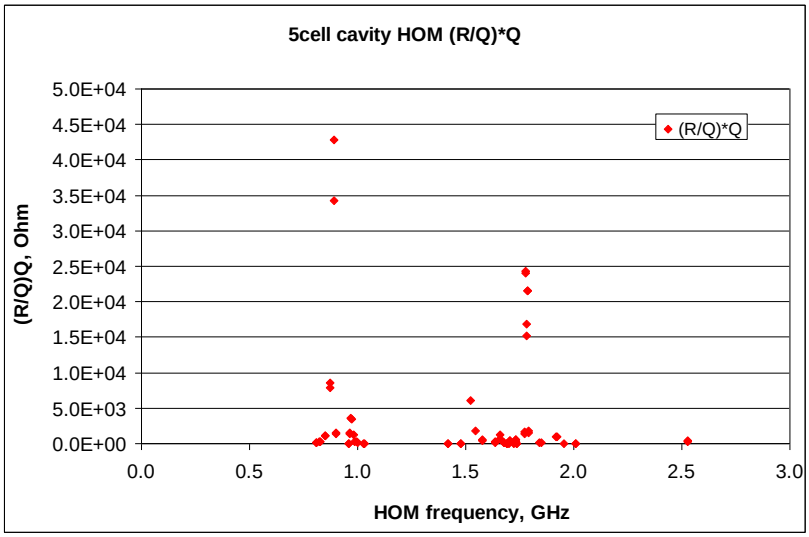

Figure 7.1. HOMs impedances in the BNL 5cell cavity: simulations and measurements.

Table 8. The 10 largest (R/Q)*Q dipole HOMs.

f, Hz	R/Q, Ohm	Q,	(R/Q)*Q
8.92E+08	57.181	7.5E+02	4.3E+04
8.89E+08	57.181	6.0E+02	3.4E+04
1.78E+09	3.3927	7.2E+03	2.4E+04
1.78E+09	3.3927	7.1E+03	2.4E+04
1.78E+09	5.1167	4.2E+03	2.1E+04
1.78E+09	5.1167	4.2E+03	2.1E+04
1.78E+09	1.6975	9.9E+03	1.7E+04
1.78E+09	1.6975	9.0E+03	1.5E+04
8.73E+08	47.013	1.8E+02	8.6E+03
8.72E+08	47.013	1.7E+02	7.8E+03

The linacs are joined together by 180 degrees arcs. Each of the arcs is presented by 4x4 transport matrix to match beta-functions between linacs. We used Twiss parameters, which are closed to optimized beta-functions in linac the entrance and exit from Table 6. The same arcs used for accelerated beam and for decelerated one hence even small difference from summitry condition at the arcs ends determinates the phase advance in the arc.

For BBU stability having the adjustable phase advance in the arcs is very important. For mirror-symmetric beta function the phase advance in the arcs can be freely adjusted to increase the BBU threshold current. We symmetrysize the beta functions by slightly changing them from the values shown in the Table.6. The beta functions and phase advance in all 6 arcs during acceleration are presented in the Table 9. For the deceleration stage we used the same arcs in the reverse order.

Table 9. Twiss parameters in the arcs used for BBU simulation.

Arc name	Phase Advance, rad	Beta entrance, m	Alpha entrance	Beta exit, m	Alpha exit
Arc1.1	1.127	847.2	-1.535	847.2	1.535
Arc1.2	1.071	910.35	-1.685	910.35	1.685
Arc2.1	1.074	933.2	-1.71	933.2	1.71
Arc2.2	1.055	920.7	-1.72	920.7	1.72
Arc3.1	1.052	921.95	-1.725	921.95	1.725
Arc3.2	1.086	922.2	-1.68	922.2	1.68

In order to test the BBU threshold sensitivity to the path length (i.e. the frequency and the time of flight) we performed additional studies. We used the same arcs optics and linacs configuration with different path lengths, which were changed by plus or minus one RF wavelength.

Our studies showed that 0.5% spread of HOM frequency is sufficient to reach 12 to 25 mA threshold current for different path lengths. In all scenarios practical scenarios with HOM frequency exceeding 0.2% the BBU threshold current is well above required operational current of 6 mA. The results of our studies are summarized in Fig. 7.2.

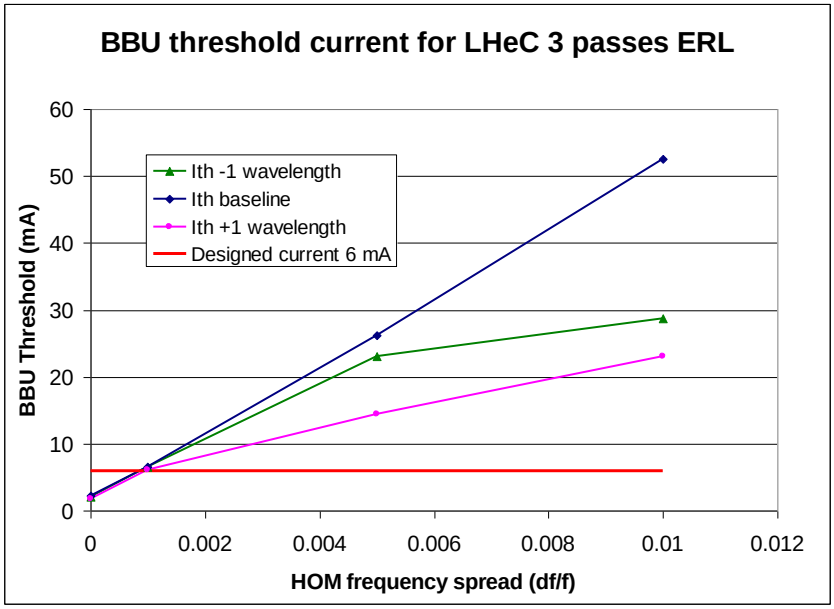

Figure 7.2. Simulation results for LHeC BBU threshold using GBBU [1] as a function of the HOM frequency spread.

Based on current understanding the BBU phenomena, one can conclude that there are no showstoppers to use the simple linac design without quadrupoles for LHeC ERL.

Conclusions

A 60-GeV 3-pass ERL is an excellent choice for accelerating polarized electrons in a high-luminosity LHeC. We have discussed arc optics design, linac cryomodule, splitters and combiners, overall layout, compensation schemes for synchrotron-radiaton energy losses, u coherent energy loss from resistive wall and coherent synchrotron radiation, and simulations of beam break up as a function of HOM frequency spread. Our studies of main beam-dynamics issues did not indicate any showstoppers. There are two possible scenarios for compensating the synchrotron-radiation energy losses, which either use a higher-harmonic RF system or optimize the beam phases in the main linacs.

References

[1] E. Pozdeyev, Phys. Rev. ST Accel. Beams, 054401 (2005).

Appendix A. Compensating for SR by the main linacs [2]

This is very brief description of how equations can be solved and the solution can be found for compensating losses of the energy in individual arcs. Here formulae are written for LHeC ERL case. These general formulae assume possibility of two different arcs. In the case of the LHeC ERL the arcs are nearly identical $\varepsilon_1(E)=\varepsilon_2(E)$.

Start from known E_i and linac gains and finish with E_{max}

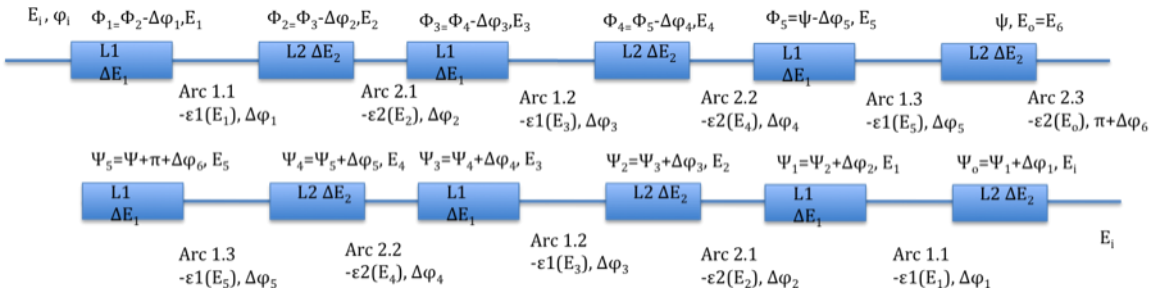

We know φ_1, E_i and energy gains in linacs. $\varepsilon_1(E)$, $\varepsilon_2(E)$ are (energy dependent) energy losses in each arc.

Step 1

$$\begin{aligned} &E_1 = E_i + \cos(\varphi_1) = E_i + \alpha\cdot\cos(\psi_0) + \varepsilon_1(E_i + \cos(\varphi_1));\\ &\cos(\varphi_1) - \alpha\cos(\psi_0) = \varepsilon_1(E_i + \cos(\varphi_1)) \end{aligned} \tag{1}$$

It may have solution for ψ_0, which will determine

$$E_1 = E_i + \cos(\varphi_1); \tag{2}$$

Step 2 $\varphi_2 = \varphi_1 + \Delta\varphi_1;\ \psi_1 = \psi_0 - \Delta\varphi_1.$

$$\begin{aligned} &E_2 = E_1 + \alpha\cdot\cos(\varphi_1 + \Delta\varphi_1) - \varepsilon_1(E_1)\\ &E_2 = E_1 + \cos(\psi_0 - \Delta\varphi_1) + \varepsilon_2(E_1 + \alpha\cdot\cos(\varphi_1 + \Delta\varphi_1) - \varepsilon_1(E_1));\\ &\alpha\cdot\cos(\varphi_1 + \Delta\varphi_1) - \cos(\psi_0 - \Delta\varphi_1) = \varepsilon_1(E_1) + \varepsilon_2(E_1 + \alpha\cdot\cos(\varphi_1 + \Delta\varphi_1) - \varepsilon_1(E_1)) \end{aligned} \tag{3}$$

It may have solution for $\Delta\varphi_1$, which will determine

$$E_2 = E_1 + \alpha\cdot\cos(\varphi_1 + \Delta\varphi_1) - \varepsilon_1(E_1),\ \varphi_2 = \varphi_1 + \Delta\varphi_1;\ \psi_1 = \psi_0 - \Delta\varphi_1. \tag{4}$$

Step 3 $\varphi_3 = \varphi_2 + \Delta\varphi_2;\ \psi_2 = \psi_1 - \Delta\varphi_2.$

$$\begin{aligned} &E_3 = E_2 + \cos(\varphi_2 + \Delta\varphi_2) - \varepsilon_2(E_2)\\ &E_3 = E_2 + \alpha\cdot\cos(\psi_1 - \Delta\varphi_2) + \varepsilon_1(E_2 + \cos(\varphi_2 + \Delta\varphi_2) - \varepsilon_2(E_2));\\ &\cos(\varphi_2 + \Delta\varphi_2) - \alpha\cdot\cos(\psi_1 - \Delta\varphi_2) = \varepsilon_2(E_2) + \varepsilon_1(E_2 + \cos(\varphi_2 + \Delta\varphi_2) - \varepsilon_2(E_2)) \end{aligned} \tag{5}$$

It may have solution for $\Delta\varphi_2$, which will determine

$$E_3 = E_2 + \cos(\varphi_2 + \Delta\varphi_2) - \varepsilon_2(E_2),\ \varphi_3 = \varphi_2 + \Delta\varphi_2;\ \psi_2 = \psi_1 - \Delta\varphi_2. \tag{6}$$

Step 4 $\varphi_4 = \varphi_3 + \Delta\varphi_3;\ \psi_3 = \psi_2 - \Delta\varphi_3.$

$$\begin{aligned} &E_4 = E_3 + \alpha\cdot\cos(\varphi_3 + \Delta\varphi_3) - \varepsilon_1(E_3) \\ &E_4 = E_3 + \cos(\psi_2 - \Delta\varphi_3) + \varepsilon_2(E_3 + \alpha\cdot\cos(\varphi_3 + \Delta\varphi_3) - \varepsilon_1(E_3)); \\ &\alpha\cdot\cos(\varphi_3 + \Delta\varphi_3) - \cos(\psi_2 - \Delta\varphi_3) = \varepsilon_1(E_3) + \varepsilon_2(E_3 + \alpha\cdot\cos(\varphi_3 + \Delta\varphi_3) - \varepsilon_1(E_3)) \end{aligned} \tag{7}$$

It may have solution for $\Delta\varphi_1$, which will determine

$$E_4 = E_3 + \alpha\cdot\cos(\varphi_3 + \Delta\varphi_3) - \varepsilon_1(E_3),\ \varphi_4 = \varphi_3 + \Delta\varphi_3;\ \psi_3 = \psi_2 - \Delta\varphi_3. \tag{8}$$

Step 5 $\varphi_5 = \varphi_4 + \Delta\varphi_4;\ \psi_4 = \psi_3 - \Delta\varphi_4.$

$$\begin{aligned} &E_5 = E_4 + \cos(\varphi_4 + \Delta\varphi_4) - \varepsilon_2(E_4) \\ &E_5 = E_4 + \alpha\cdot\cos(\psi_3 - \Delta\varphi_4) + \varepsilon_1(E_4 + \cos(\varphi_4 + \Delta\varphi_4) - \varepsilon_2(E_4)); \\ &\cos(\varphi_4 + \Delta\varphi_4) - \alpha\cdot\cos(\psi_3 - \Delta\varphi_4) = \varepsilon_2(E_4) + \varepsilon_1(E_4 + \cos(\varphi_4 + \Delta\varphi_4) - \varepsilon_2(E_4)) \end{aligned} \tag{9}$$

It may have solution for $\Delta\varphi_2$, which will determine

$$E_5 = E_4 + \cos(\varphi_4 + \Delta\varphi_4) - \varepsilon_2(E_4),\ \varphi_3 = \varphi_2 + \Delta\varphi_2;\ \psi_2 = \psi_1 - \Delta\varphi_2. \tag{10}$$

Step 6 $\psi = \varphi_5 + \Delta\varphi_5;\ \psi_5 = \psi_4 - \Delta\varphi_5.$

$$\begin{aligned} &E_6 = E_5 + \alpha\cdot\cos(\varphi_5 + \Delta\varphi_5) - \varepsilon_1(E_5) \\ &E_6 = E_5 + \cos(\psi_4 - \Delta\varphi_5) + \varepsilon_2(E_5 + \alpha\cdot\cos(\varphi_5 + \Delta\varphi_5) - \varepsilon_1(E_5)); \\ &\alpha\cdot\cos(\varphi_5 + \Delta\varphi_5) - \cos(\psi_4 - \Delta\varphi_5) = \varepsilon_1(E_5) + \varepsilon_2(E_5 + \alpha\cdot\cos(\varphi_5 + \Delta\varphi_5) - \varepsilon_1(E_5)) \end{aligned} \tag{11}$$

It may have solution for $\Delta\varphi_1$, which will determine

$$E_6 = E_5 + \alpha\cdot\cos(\varphi_5 + \Delta\varphi_5) - \varepsilon_1(E_5),\ \psi = \varphi_5 + \Delta\varphi_5;\ \psi_5 = \psi_4 - \Delta\varphi_5. \tag{12}$$

Also it defines the last pass phase advance:

$$\Delta\varphi_6 = \pi - \psi + \psi_5$$

[2] Using main linacs to compensate for synchrotron radiation losses in high energy ERLs, Vladimir N. Litvinenko, in submission process